Advanced Materials Research
ISSN: 1662-8985, Vol. 1170, pp 1-10
doi:10.4028/p-0612s4

Submitted: 2021-07-07
Revised: 2021-12-08
Accepted: 2021-12-14
Online: 2022-04-19

Surface Defect Classification in Silicon Wafer Manufacturing Using the Linear-Based Channeling and Rule-Based Binning Algorithms

Hao Hu[1,a*], Kari Ullakko[1,b], Mingming Chao[2,c] , Xin Lai[2,d]

[1]Lappeenranta-Lahti University of Technology, Finland

[2]Advanced Silicon Technology Co., Ltd. China

[a]huha0002@e.ntu.edu.sg, [b]kari.ullakko@lut.fi, [c]mmchao@ast.com.cn, [d]xlai@ast.com.cn

Keywords: Process-induced defects, Surface-adhered foreign particles, Crystal-originated pits, Scanning surface inspection systems, Defect classification, Localized light scatterers

Abstract. Developing an accurate means of classifying defects, such as crystal-originated pits, surface-adhered foreign particles, and process-induced defects, using scanning surface inspection systems (SSIS) is of paramount importance because it provides the opportunity to determine the root causes of defects, which is valuable for yield enhancement. This report presents a novel defect classification approach developed by optimizing the linear-based channeling (LBC) and rule-based binning (RBB) algorithms that are applied to a commercially available SSIS (KLA-SP5), in combination with test sample selection including the signature defect patterns associated with the typical crystal growth process. The experimental results demonstrate that defect classification is possible with an accuracy and purity above 80% using the LBC algorithm and 90% using the RBB algorithm.

Abbreviations

Scanning surface inspection system (SSIS)
Crystal-originated pits (COP)
Surface-adhered foreign particles (SFP)
Process-induced defects (PID)
Linear-based channeling (LBC)
Rule-based binning (RBB)
Light point defects (LPD)
Non-cleanable light point defects (LPDN)
Localized light scatterer (LLS)

1. Introduction

Highly pure crystalline silicon (Si) wafers are used in the semiconductor industry as the basis for manufacturing electronic devices, owing to silicon's beneficial structure, satisfactory mechanical strength, and favorable chemical and electrical properties. Defects on the surface of such wafers may be generated during the various manufacturing steps. These surface defects are generally classified into three categories, according to their source during the silicon wafer manufacturing process [1,2],

- Crystal grown-in defects, such as crystal-originated pits (COP): These are voids in the bulk crystal that are delineated as pits on the wafer surface. They are captured as non-cleanable light point defects (LPDN) on the wafer surface by the scanning surface inspection systems (SSIS). These defects have the greatest negative impact on the device performance - for example, they lead to gate-oxide-integrity failure [3–5].
- Surface-adhered foreign particles (SFP): These are organic particles or metal contaminants generated by human activities, fabrication facilities, equipment, and processes [6–8]. The contemporary silicon wafer manufacturing process has been carefully designed to control the

deposition of organic particles and metal contaminants, for eliminating their impact on the device performance. SFP are often captured as light point defects (LPD) by SSIS.

- Process-induced defects (PID): These are also called polishing-induced defects. These include all the unwanted imperfections generated from the manufacturing processes, particularly during polishing, such as residues, stains, dimples, scratches, and surface particles. PID are responsible for gate dielectric failures during the device fabrication process and are observed as either LPD or LPDN by SSIS [9–11].

These surface defects are detrimental for the electronic devices made on the Si wafers. Therefore, Si wafer manufacturing requires tight defect control. This is achieved by using highly sensitive metrology tools for detecting the surface defects [12,13] and elaborate algorithms for classifying them. Effectively using the linear-based channeling (LBC) and rule-based binning (RBB) algorithms applied to commercially available SSIS such as the KLA-SP5 [14], will enable the appropriate categorization of defects during the defect classification process. In the system, two darkfield angles of incidence (oblique and normal) and two darkfield collectors (wide and narrow), in addition to a brightfield subsystem (differential interference contrast) comprise the data channels for collecting surface defect information [15]. As illustrated in Figure 1, there are several defect characteristics such as the size information of the darkfield wide (DW) and darkfield narrow (DN) channels, size information of the normal DW and DN channels, signal to noise ratio (SNR), and positions of the oblique and normal light incidences. The LBC algorithm uses the result of the cross-channel ratio for discriminating particles and defects on silicon wafers [16]. The RBB algorithm does not simply apply the ratios of defect sizing by various channels. It is a combination of defect characteristics including the information for the LBC algorithm, the attributes for differential interference contrast (DIC) such as size, polarity, defect location (x-y positions), and other general information including the aspect ratio, length, and area. [17]. The present paper presents a report about an investigation about the effective of such algorithms provided by a commercially available SSIS. Experimental details are presented in section 2 and the results are discussed in section 3 before the report is closed by a section with a summary and conclusions.

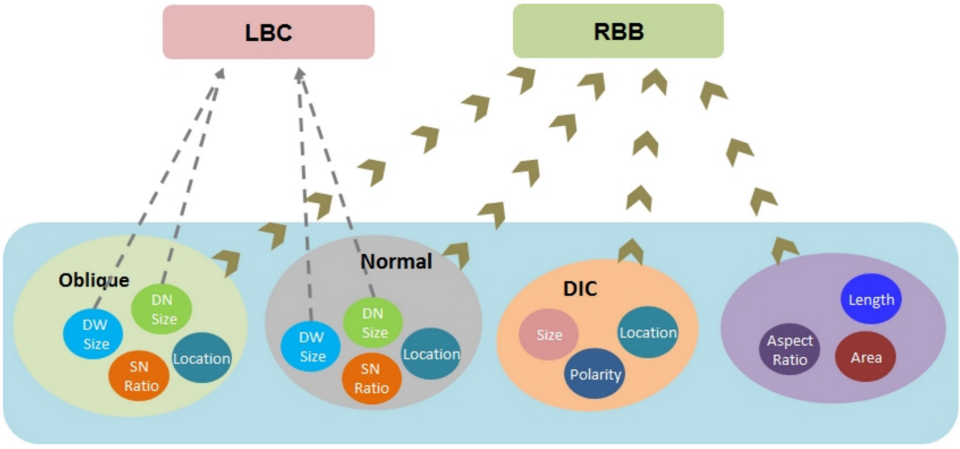

Fig. 1 Surface defect characteristics that applied in the LBC and RBB algorithms.

2. Experimental Details

2.1 Defect Engineering Flow and Preliminary Investigations

There are five steps involved during process control and defect engineering, for which corresponding surface defect metrology is selected (Figure 2).

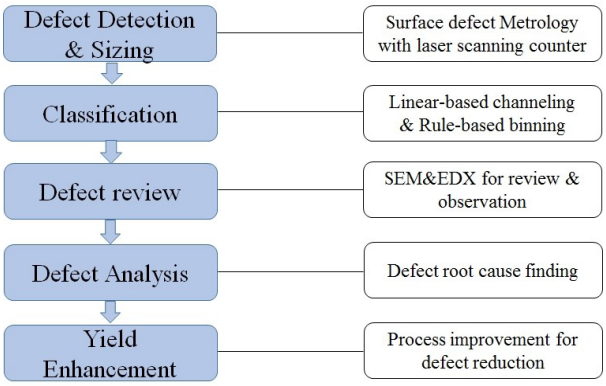

Fig. 2 Overview of the defect engineering flow for detecting and identifying the surface defects - from “defect detection & sizing” to “yield enhancement”.

Defect detection and sizing involve the use of an SSIS. In such a system a focused laser beam spot is scanned across the wafer surface and the scattered light is collected by an optical system and fed into one or more detectors. The detector(s) signal(s) are recorded as a function of the spot position on the wafer surface. Any signal above a threshold close to the background, which is generated by the overall surface roughness, is considered to result from a surface defect, called in general LLS (localized light scatterer). In the current investigation an SSIS provided from KLA is used, the KLA-SP5 (Figure 3). This tool is equipped with two collectors or channels DN and DW. The channel DN collects light scattered close to the surface normal whereas the channel DW covers a large solid angle of scattered light. The intensity of the light scattered by an LLS depends on the refractive index, shape, and size of the LLS. An equivalent size expressed as umLSE or nmLSE is assigned to the LLSs by calibrating the SSIS with polystyrene latex spheres of different diameters, deposited on a reference silicon wafer surface [18–20]. The acronym “LSE” (latex sphere equivalent or light scattering equivalent) [21] added to the length unit indicates that the size reported by the SSIS is a metric for the light scattering cross section of the LLS and not for the true geometrical size.

In addition, SP5 provides the option of different incidence angles of the laser beam. The user of the SP5 may choose between incidence perpendicular to the wafer surface (normal incidence) or incidence under an angle of 5° , 20° , 25° or 72° (oblique incidence). A brightfield subsystem based on DIC comprise the data channels for collecting surface defect information [15].

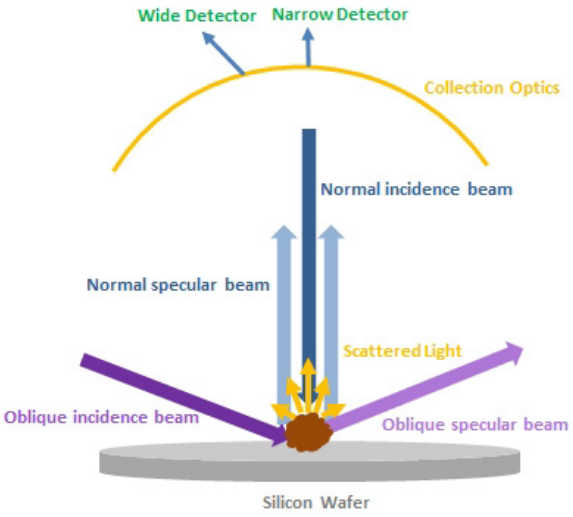

Fig. 3 Schematic overview of the KLA-SP5 surface scanning counter-dark-field inspection based on light scattering technology (oblique and normal incidence beam, oblique and normal specular beam, and a wide and narrow detector).

Defect classification, which is the key focus of this study, is a crucial step in defect engineering flow. The output of the various channels and illumination options is the basic for the algorithms used for classifying the surface defects (Fig. 1). LBC and RBB are efficient defect classification algorithms that are used by SSIS. LBC uses the cross-channel size ratio n (Equation 1), where DN denotes equivalent size of a defect as captured by the narrow channel, whereas DW denotes the size of the same defect as measured by the wide channel. Using LBC, surface defects are classified into LPD and LPDN based on the cross channel ratio n where LPDN typically display an n > 1. RBB also applies the concept of the cross-channel size ratio, however, it cascades the classification process to introduce multi-level channeling. Particularly, it allows the area feature (radial or box) – to be positioned for predefining defects of interest (DOI).

$$n = f(DN, DW) = {}^{DN}/_{DW} \tag{1}$$

For being able to correctly classify LLS by LBC and RBB it is necessary to set up the parameters of these algorithms appropriately. This is achieved by reviewing the LLS with scanning electron microscopy (SEM), which is a labor intensive and time-consuming method that is only suitable as a verification process for DOI with known x-y coordinates on the sample wafer. In addition, SEM is a destructive method. Classification and reviewing of defects are often iterative processes that optimize the defect classification results. The LLS captured by the SSIS comprising LPD (e.g., particles, flakes, residues, stains, and spheres) and LPDN (e.g., COP, embedded defects, bumps, pits/dents, dimples, scratches, faint lines, and gouges), were reviewed using SEM KLA-eDR7380 in the current investigation, examples are displayed in Figure 4. Reviewing defects to identify DOI is an effective step toward determining the root causes of defects.

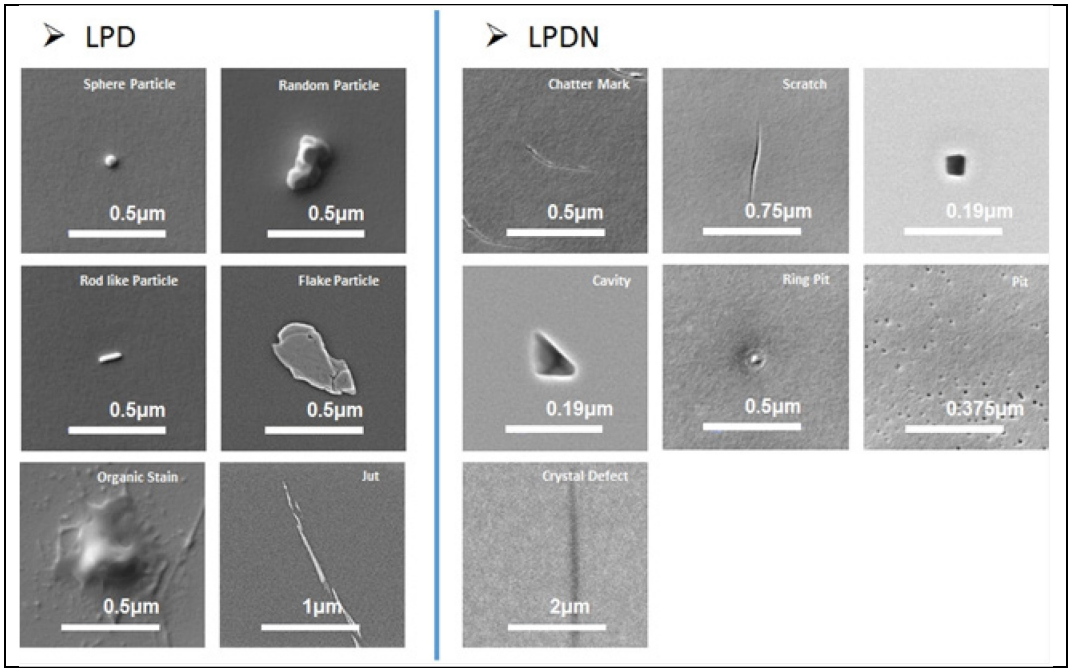

Fig. 4 LPD and LPDN high-resolution 2D images captured by SEM.

Defect analysis includes SEM studies for reviewing defect topographies, EDX studies for elemental analysis of particles, and a root cause analysis for the inline manufacturing processes. By identifying the root cause of the surface defects, process engineers can understand and reduce PID for continuous process improvement. Yield enhancement is an important goal of defect engineering, which is realized by improving individual processes as well as the overall operation [13,21,22].

2.2 Challenges and the goal of defect classification

Surface defects are captured as LLS and classified as LPD and LPDN when using the LBC algorithm applied in the SSIS, with a typical setting of a cross-channel ratio threshold rth for n with $1.10 < rth < 1.30$ by which LPD and LPDN are distinguished. The situation is shown schematically in Figure 5. Based on the LBC algorithm, the defects may be classified into two groups: One group consists of SFP and PID, and the other group of COP. Therefore, the LBC algorithm with the single-level channeling is not expected to efficiently distinguishing the SFP and PID. In contrast, the RBB algorithm is expected to classify the SFP, PID, and COP efficiently using the multiple-level channeling that involves defect characteristics such as the defect location, DIC information, the aspect ratio, length, and area. The blank areas in Figure 5, where the circles overlap, indicate the uncertain defect classification among the three defect sources. The task for being able to apply the algorithms in a wafer production line is to minimize the uncertain sectors by tuning the parameters of these algorithms. The next section describes how this was successfully achieved.

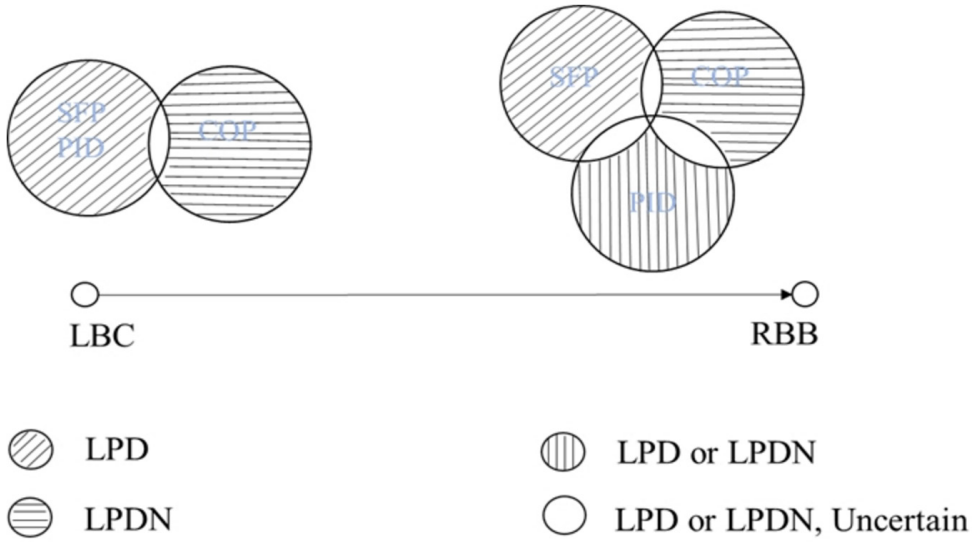

Fig. 5 Schematic view of defect classification implemented using the LBC and RBB algorithms – Categorization into SFP, COP, and PID is based on the source of defects; categorization into LPD and LPDN is according to the SSIS equipment (KLA-SP5).

3 Results and Discussion

The investigation regarding to the classification accuracy and purity was performed in two steps. In the first step specifically selected wafers were used for determining the appropriate parameters for the LBC and RBB algorithms. In the second step, subsequently then a set of production wafers was measured and analyzed with the such defined parameters. In both steps the results of the SSIS measurement were cross-checked with SEM investigation of the defects found.

In the first step two groups (5 wafers each) of p-type, lightly doped, and mirror-polished silicon wafers with a 300 mm diameter, (100) crystal orientation, and 775±5 µm thickness were selected for the experiments. In particular, the COP density and distribution of the two groups of wafers were analyzed to investigate the results obtained using LBC and RBB. Group 1 (5 wafers) consisted of COP-free wafers, in which the defect type of LPD dominated according to the SSIS used with $n < rth$. Therefore, the LLS on the wafer surface, which were classified as LPD by the KLA-SP5, primarily contribute to the defect counts. Group 2 (5 wafers) consisted of COP-dominated/COP-rich wafers which exhibited the characteristic disk and ring pattern of COP [23,24]. By this it is possible to apply RBB (radial positioning) to optimize the accuracy of defect classification [6,25]. The LBC algorithm was applied to both groups of wafers in order to tune the cross-channel ratio according to the DN and DW signals from the oblique and normal incident lights. Subsequently, the RBB

algorithm was applied to wafer group 2 with respect to the information regarding the defect location, aspect ratio, size, polarity of the DIC signal, length, and defect area.

Following the experiments, we selected one premium production lot (25 wafers) and ran through it using the qualified KLA-SP5 system. The defect classification result was verified by SEM (KLA-eDR7380) using the confusion matrix technique [11]. The accuracy and purity were reported accordingly.

The surface defects captured by the surface scanning counter are randomly distributed on the Group 1 wafers, as shown in Figure 6. Most of the LPD detected by KLA-SP5 and reviewed by the SEM are process-induced. Moreover, some SFP are also accurately classified as LPD. Notably, crystal grown-in defect patterns, in terms of defect sizing, density, and distribution, were not observed. The distribution of point defects varies from 30 to 145 mm across the radial direction of the wafer, as shown in Figure 7 (defect count versus radius). Under this scenario, we can apply the LBC algorithm in the defect classification process because zero grown-in defects were observed in the prime grade of COP-free single crystalline silicon. Therefore, the key focus of the surface defects is LLS that are generated by PID and SFP during silicon wafer manufacturing.

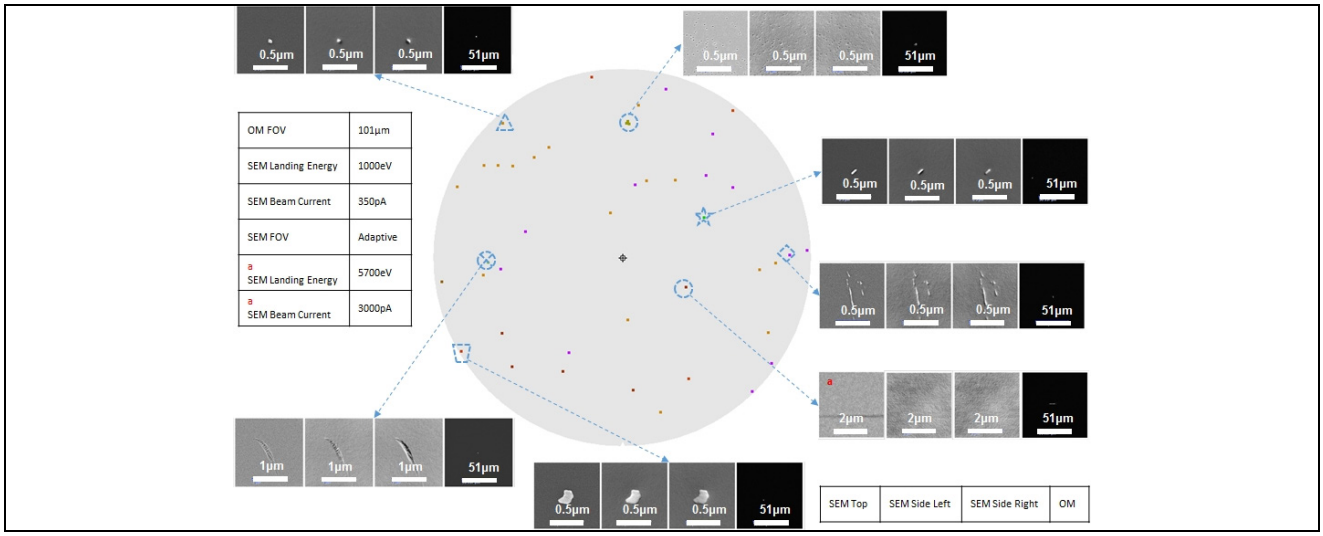

Fig. 6 Defect classification using LBC for COP-free single crystal silicon wafer. There is no specific pattern of defect distribution. PID dominated the defect map.

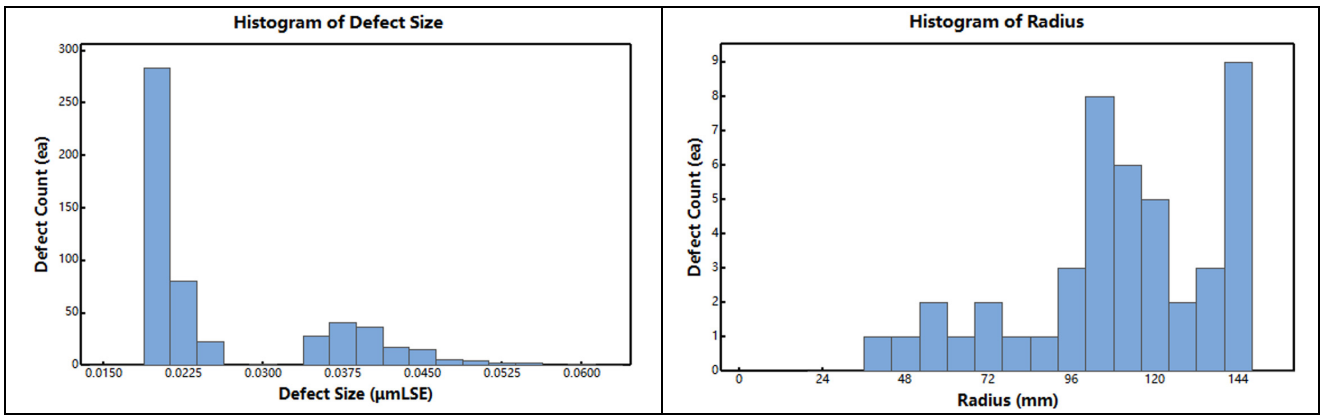

Fig. 7 Size and density distribution of defects in the COP-free wafers.

The results of Group 2 wafers, silicon wafers with the signature COP defect distributions (disk and ring patterns at the center and edges, respectively), are shown in Figure 8 and 9. The radially varying COP distribution is aligned to the radial dependence of the vacancy concentration [23]. Based on this observation, the COP are distributed at the central area from 0 to 50 mm and close to

the edge of the wafer at radii from 105 to 145mm. The COP size distribution also indicates the radial position. This indicates that smaller sized COP (<0.026 µmLSE) display higher densities at the edge area, whereas larger COP (>0.032 µmLSE) show lower densities at the central area of the wafer (0 to 50 mm). In contrast to other studies on surface defect classification [9,26], we defined two areas with COP - one was the disk-shaped center area (within the 0 - 50 mm radius) and the other was the ring-shaped edge area (within the 105 -145 mm radius). The defects in these areas are thus classified as LPDN based on the distribution of the crystal grown-in defects. In contrast, the PID and SFP are captured as LPD in the exclusion area of the DOI. In this experiment, limited LPD were observed based on the detection limit (DL) of 0.022 µmLSE.

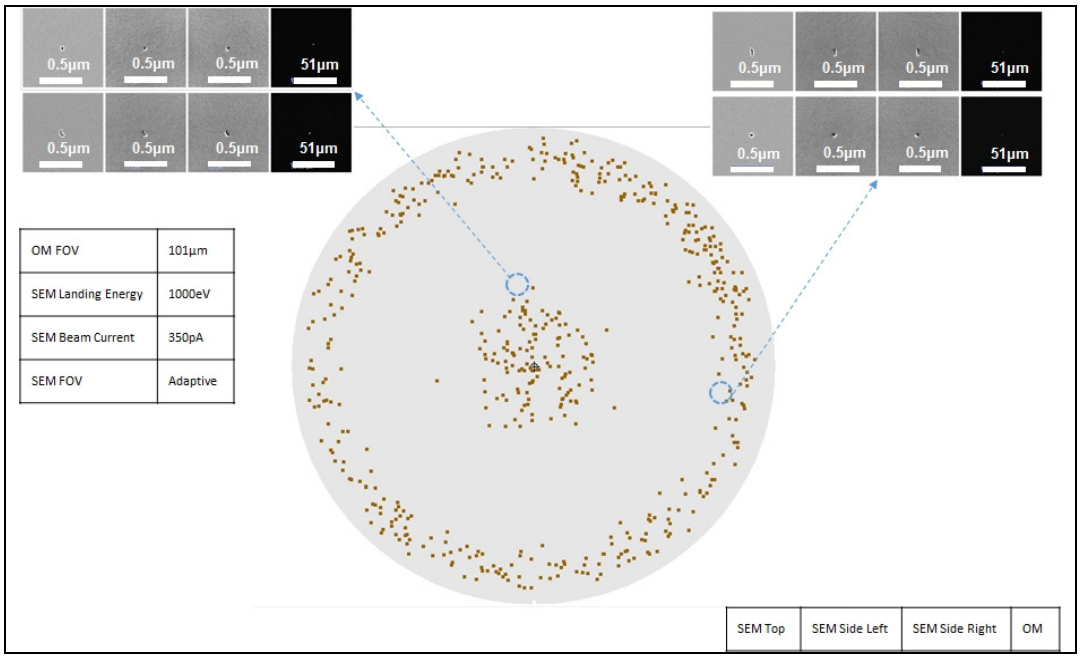

Fig. 8 Defect classification using RBB for the signature COP single crystal silicon wafer. Applying defect characteristics such as position, aspect ratio, and area for discriminating surface defects.

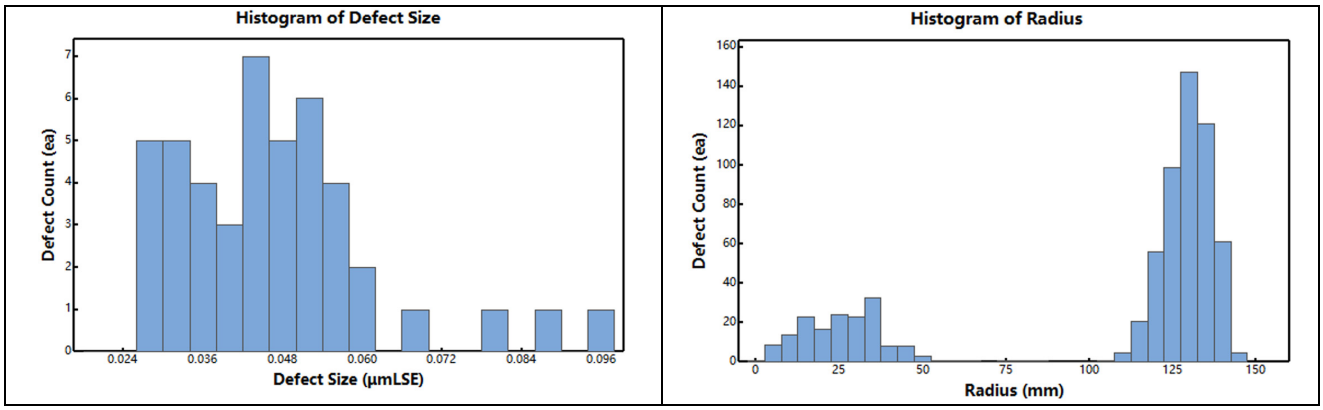

Fig. 9 Size and density distribution of defects in the signature COP sample for the second experiment.

In the second step, in order to evaluate the defect classification performance of the KLA-SP5 using the LBC and RBB algorithms, a premium production lot of 25 wafers was measured and reviewed. Comparing the result of the KLA-SP5 and the KLA-eDR7380, the accuracy and purity of the classification are calculated based on the Equation 2 and 3 using the confusion matrix technique [11]. The results are reported in Table 1 and 2. Table 1 lists the results where only the LBC algorithm was applied and the accuracy and purity were above 80%. However, it is reasonably accepted, that this approach is usually not able to distinguish the SFP and PID efficiently (grouping

the SFP and PID as one). As shown in Table 2, using the RBB algorithm the defects are efficiently classified as SFP, PID, and COP and the accuracy and purity are above 90%. This is sufficient to capture excursion wafers based on practical experience [11].

Accuracy (%) = Total correctly classified by SSIS/ Total classified by SEM (2)
Purity (%) = Total correctly classified by SSIS/ Total classified by SSIS (3)

Table 1 Results of defect classification using LBC only based on a confusion matrix (accuracy and purity).

		SEM Review		
		SFP+PID	**COP**	**Purity**
SSIS	**SFP+PID**	500	56	89.9%
	COP	34	248	87.9%
	Accuracy	93.6%	81.6%	

Table 2 Results of defect classification using RBB based on a confusion matrix (accuracy and purity).

		SEM Review			
		SFP	**COP**	**PID**	**Purity**
SSIS	**SFP**	140	6	8	90.9%
	COP	8	260	14	92.2%
	PID	7	12	255	93.1%
	Accuracy	90.3%	93.5%	92.1%	

Therefore, in this study, the LBC and RBB algorithms were quantitatively evaluated considering one specific scenario. Other scenarios might be worth studying, including cases where only disk-shaped or ring-shaped defect patterns are observed at the center or the edges, respectively, for efficiently streamlining the troubleshooting process. Designing suitable scenarios for such studies requires a proper understanding of the silicon crystal growth conditions, such as the interface shape of crystal-melt, pulling speed, and temperature gradient [27]. Characterizing the silicon crystal in terms of crystal type, defect density, and size distribution prior to defect classification is a preliminary requirement [28,29]. This novel method works well in silicon wafer manufacturing, specifically for manufacturing large wafers.

4 Summary and Conclusions

It was demonstrated that LBC and RBB algorithms are able to distinguish COP, SFP and PID with a high success rate by using a commercially available SSIS, provided the algorithms are appropriately set up. For establishing appropriate parameter settings for the algorithms two sets of specifically selected wafers were used. The results show that it is essential to obtain grown-in defect information and to select the appropriate samples for the LBC and RBB setup in the SSIS. In addition, this approach is applicable for acquiring defect information during the manufacturing

processes, such as special process-induced patterns on the surfaces and edges of the wafers, thus opening opportunities for future studies.

CRediT authorship contribution statement

Hao Hu: Investigation, Writing, Project administration. **Kari Ullakko**: Writing-Review, Supervision. **Mingming Chao**: Investigation. **Xin Lai**: Investigation.

References

[1] R.F. Reinhardt, K.A., Reidy, Handbook of Cleaning for Semiconductor Manufacturing, John Wiley and Sons, New Jersey, 2011.

[2] V. Lindroos, M. Tilli, A. Lehto, T. Motooka, Handbook of Silicon Based MEMS Materials and Technologies (Micro and Nano Technologies), William Andrew, 2010.

[3] J. Park, K. Kwack, Crystal Originated Particle Induced Oxide Breakdown in Czochralski Silicon Wafer, J. Korean Phys. Soc. 38 (2001) 356–365.

[4] M. Hourai, E. Asayama, H. Nishikawa, M. Nishimoto, T. Ono, M. Okui, Recognition and Imaging of Point Defect Diffusion, Recombination, and Reaction During Growth of Czochralski-Silicon Crystals, J. Electron. Mater. 49 (2020) 5110–5119. https://doi.org/10.1007/s11664-020-08203-w.

[5] G. Kissinger, J. Dabrowski, T. Sinno, Y. Yang, D. Kot, A. Sattler, Ab initio calculations and rate equation simulations for vacancy and vacancy-oxygen clustering in silicon, J. Cryst. Growth. 468 (2017) 424–432. https://doi.org/10.1016/j.jcrysgro.2016.10.073.

[6] B. Jean-Luc, D. Bruno, Contamination Monitoring and Analysis in Semiconductor Manufacturing, in: Semicond. Technol., Semiconductor Technologies, 2010: pp. 57–78. https://doi.org/10.5772/8561.

[7] A. Nutsch, B. Beckhof, G. Bedana, G. Borionetti, D. Codegoni, S. Grasso, G. Guerinoni, A. Leibold, M. Müller, M. Otto, L. Pfitzner, M.L. Polignano, D. De Simone, L. Frey, Characterization of organic contamination in semiconductor manufacturing processes, AIP Conf. Proc. 1173 (2009) 23–28. https://doi.org/10.1063/1.3251227.

[8] K. Reinhardt, W. Kern, Handbook of Silicon Wafer Cleaning Technology, William Andrew, 2018.

[9] H. Ohta, S.M. Byeong, G.P. Jea, H.L. Sang, H.A. Jeong, H. Kwon, T. Watanabe, K. Ichinose, K. Nemoto, K.P. Sung, Quantifying yield impact of polishing induced defect on the silicon surface, ASMC (Advanced Semicond. Manuf. Conf. Proc. (2009) 41–45. https://doi.org/10.1109/ASMC.2009.5155950.

[10] R. Vos, K. Xu, M. Lux, W. Fyen, R. Singh, Z. Chen, P. Mertens, Z. Hatcher, M. Heyns, Use of surfactants for improved particle performance of dHF-based cleaning recipes, Solid State Phenom. 76–77 (2001) 263–266. https://doi.org/10.4028/www.scientific.net/SSP.76-77.263.

[11] Y.Y. Lin, F.S. Tsai, L.C. Hsu, H.K. Hsu, C.Y. Li, Y.Y. Ke, C.W. Huang, J.M. Chen, S.J. Chang, T.Y. Lee, E. Chen, C.Y. Cheng, Fast and accurate defect classification for CMP process monitoring, ASMC (Advanced Semicond. Manuf. Conf. Proc. 2019-May (2019) 224–228. https://doi.org/10.1109/ASMC.2019.8791750.

[12] P. Wagner, Metrology of 300 mm silicon wafers: Challenges and results, 1998 Int. Conf. Charact. Metrol. ULSI Technol. 153 (1998) 153–160. https://doi.org/10.1063/1.56790.

[13] A. Zandiatashbar, B. Kim, Y. Yoo, K. Lee, A. Jo, J.S. Lee, S.-J. Cho, S. Park, High-throughput automatic defect review for 300mm blank wafers with atomic force microscope, 9424 (2015) 94241X. https://doi.org/10.1117/12.2086042.

[14] M. Akbulut, H. Lihn, M. Vaez-irvani, S. Stok, G. Zhao, W. Inspection, COPs / Particles Discrimination With a Surface Scanning Inspection System, Semicond. Int. (1999) 1–8.

[15] B. Pinto, J. Saito, W. Shen, L. Cheung, A.W.K. Corporation, New Inspection Technology for 45nm Wafers, Yield Manag. Solut. (2007) 28–32.

[16] F. Passek, R. Schmolke, H. Piontek, A. Luger, P. Wagner, Discrimination of particles and defects on silicon wafers, Microelectron. Eng. 45 (1999) 191–196. https://doi.org/10.1016/S0167-9317(99)00145-8.

[17] Y. Liu, T. Wei, M. Li, Z. Li, Z. Xue, X. Wei, Characterization of grown-in defects in Si wafers by gas decoration, Mater. Sci. Semicond. Process. 130 (2021) 105822. https://doi.org/10.1016/j.mssp.2021.105822.

[18] K. Xu, R. Vos, G. Vereecke, M. Lux, W. Fyen, F. Holsteyns, K. Kenis, P.W. Mertens, M.M. Heyns, C. Vinckier, Relation between particle density and haze on a wafer: A new approach to measuring nano-sized particles, Solid State Phenom. 92 (2003) 161–164. https://doi.org/10.4028/www.scientific.net/ssp.92.161.

[19] C.R. Brundle, Full wafer particle defect characterization, in: AIP Conf. Proc., AIP, 2001: pp. 285–291. https://doi.org/10.1063/1.1354412.

[20] P. Huang, Defect mapping accuracy of KLA-Tencor Surfscan 6200, 6400, and SP1, in: AIP Conf. Proc., AIP, 2001: pp. 317–321. https://doi.org/10.1063/1.1354418.

[21] SEMI, SEMI M52-0214 Guide For Specifying Scanning Surface Inspection Systems For Silicon Wafers For The 130 nm To 11 nm, 2014.

[22] C. Kupfer, H. Roth, H. Dietrich, Defect requirements for advanced 300 mm DRAM substrates, Mater. Sci. Semicond. Process. 5 (2002) 381–386. https://doi.org/10.1016/S1369-8001(02)00137-3.

[23] R.. Brown, F. Dupret, E. Dornberger, T. Sinno, W. von Ammon, Defect engineering of Czochralski single-crystal silicon, Mater. Sci. Eng. R Reports. 28 (2002) 149–198. https://doi.org/10.1016/s0927-796x(00)00015-2.

[24] Z. Zheng, T. Seto, S. Kim, M. Kano, T. Fujiwara, M. Mizuta, S. Hasebe, A first-principle model of 300 mm Czochralski single-crystal Si production process for predicting crystal radius and crystal growth rate, J. Cryst. Growth. 492 (2018) 105–113. https://doi.org/10.1016/j.jcrysgro.2018.03.013.

[25] A. Zandiatashbar, P.A. Taylor, B. Kim, Y. Yoo, K. Lee, A. Jo, J.S. Lee, S.-J. Cho, S. Park, Studying post-etching silicon crystal defects on 300mm wafer by automatic defect review AFM, (2016) 97782P. https://doi.org/10.1117/12.2220369.

[26] K.M. Saga, US10718720B2-Semiconductor wafer evaluation method and semiconductor wafer-2020.pdf, US010718720B2, 2020.

[27] J. Vanhellemont, S. Senkader, G. Kissinger, V. Higgs, M. T, Measurement , modelling and simulation of defects in as-grown Czochralski silicon, 180 (1997) 353–362.

[28] S.H. Lee, D.W. Song, H.J. Oh, D.H. Kim, Modeling of defects generation in 300mm silicon monocrystals during czochralski growth, Jpn. J. Appl. Phys. 49 (2010). https://doi.org/10.1143/JJAP.49.121303.

[29] M.S. Kulkarni, A selective review of the quantification of defect dynamics in growing Czochralski silicon crystals, Ind. Eng. Chem. Res. 44 (2005) 6246–6263. https://doi.org/10.1021/ie0500422.